Water Harvesting Research Vol. 5, No. 1, Spring & Summer 2022, Original Paper p. 93-101

University of Birjand

10.22077/JWHR.2022.5633.1072

Simulation of Flood Flows in a River Using the Finite Element Method

Zahra Baazm[a], Ehsan Mohtashami[b], Abolfazl Akbarpour*[c]

[a]PhD student, Department of Water Engineering, Faculty of Agriculture, University of Birjand, Birjand, Iran.
[b]Assistant Professor of Civil Engineering Department, University of Birjand, Birjand, Iran.
[c]Professor of Civil Engineering Department, University of Birjand, Birjand, Iran.

*Corresponding Author, E-mail address: akbarpour@birjand.ac.ir

Received: 8 September 2022/ **Revised**: 28 October 2022/ **Accepted**: 12 November 2022

Abstract

Due to the difficulty in measurement of transverse velocity in floods, it is necessary to use appropriate models for this aim. Hydrodynamic complexity of the flow in the middle of the flood is another reason for usage of precise models. Accurate prediction of flows is very difficult due to the complexity of its nature and the lack of accurate data. Here, two-dimensional modeling of the flood has been done using the finite element method (FEM). The case study is a real field river. The achieved results from the finite element model are compared with the observational data at three stations. In order to evaluate the model performance, the root mean square error (RMSE) is calculated. The relative error and the RMSE are 0.143 and 0.229 m, respectively. This amount of value indicates the high accuracy of the proposed model. In addition, computational cost including time spending and efficiency of FEM is satisfactory and this model can be used as a good tool for flow simulation.

Keywords: Finite Elements, Flood, River, Simulation, Shallow Water Equations.

1. Introduction

The most important specification of shallow water is that the vertical dimensions of the flow compared to its horizontal case, are very small. Therefore, the distribution of depth pressure can be considered hydrostatic. These assumptions lead to considerable simplification in mathematical formulation and numerical procedure (Fread, 1985).

Flows naturally are three-dimensional and, factors such as: bed friction, boundary conditions and depth of flows, due to the changes in temperature or salinity in depth are the reasons that cause changes in the third dimension (vertical dimension). However, in many practical problems, these changes can be ignored and appropriate information can be obtained at a low cost by only using two-dimensional equations of shallow water (depth is considered as average) (Bates et al., 1994).

The application of shallow water equation should be attributed to Laplace who has many researches in this matter. Remarkable work has been done in the field of tidal currents, known as Laplace tidal equations and a special form of shallow water equations. Using numerical solution of shallow water equations returns to the use of digital computers in the late 1940s. The first numerical work in this field, was the simulation of atmospheric currents by Charney in 1950 and ocean currents by Hansen in 1956 (Vreugdenhil, 1994).

Since then, many researchers have solved various forms of this equation with different numerical methods and in different engineering applications. The developed models are mainly based on the finite difference method (FDM) and this method is still ongoing. Since the late 1960s, the finite element method known as a powerful tool in solving of partial differential equations has attracted the attention of scientists and researchers. Solving these equations by finite element method began in the early 1970s. For example, the study of Wong and his colleagues in the field of meteorology (Berger and Stockstill, 1995).

Since then, many models have been developed in order to solve shallow water equations by finite element method. For example, the study of Berger and Stockstill (1995) provide a model for investigation of high-velocity flows in channels (Berger and Stockstill, 1995). Abril (2002) presented a quasi-two-dimensional mathematical model for hydraulic analysis of flow in multiple sections with straight path. The analytical solution of this model is more complex than the Shiono and Knight model and therefore, its application is limited to only rivers (Abril, 2002). Ayubzadeh and Zahiri (2003) also used the analytical solution of the Quasi-Two-Dimensional model of Shiono and Knight (1991) to simulate the hydraulic flow in the Minab River (Ayyoubzadeh and Zahiri, 2003). Barzegaran et al. (2017), used reinforced Riemann method for simulation of bed sediment. They found their results satisfactory. Khorashadizadeh et al. (2018) carry out the sensitivity analysis of finite volume shallow water model with RSA method, and find that RSA role as an efficient method for this aim.

Ghobadian and Mehrmousavi (2019) used a numerical simulation for solving shallow water equations in two-dimensional condition. Deymevar and Akbarpour (2017) modeled dam failure with using meshless local Petrov-Galerkin with solving shallow water equations. They only simulate surface water without comparison with analytical and observational results, as they noted there is no analytical relation for their problem.

Behzadi and Newman (2020) used a numerical model based on a semi-discrete Streamline Upwind Petrov–Galerkin scheme for solving shallow water equations with arbitrary bed topography and wetting–drying fronts. The proposed model is verified through well-known test cases including the traditional dam break problem, evolution of a dam break wave over an obstacle, and oscillation of a bead of water in a parabolically-shaped basin. The acquired results presented the good performance of the model.

Izem and Seaid (2021) presented a well-balanced Runge-Kutta discontinuous Galerkin method for the numerical solution of multilayer shallow water equations with mass exchange and non-flat bottom topography. The accuracy of the proposed model is examined for several examples of multilayer free-surface flows over both flat and non-flat beds. The performance of the method is also demonstrated by comparing the results obtained using the proposed method to those obtained using the incompressible hydrostatic Navier-Stokes equations, and it was accurate.

A review of the researchers' studies shows that the use of analytical solution of quasi-two-dimensional mathematical model in irregular natural rivers has many limitations or does not exist (Deymevar and Akbarpour, 2017). However, the finite element numerical method has some errors in a river with irregular boundaries, but it is more efficient and accurate than traditional models.

In this study, a 2D modeling of floodplain flow is used by finite element method. Although, this method has some limitation in cases with complicated geometry, but still accurate and stable in solving procedure. FDM is going to apply in a river case with irregular geometry in order to simulate the movement of shallow water.

2. Material and methods

2.1. Governing Equation

The TELEMAC-2D code solves the second-order partial differential equations for the average fluid flow rate (shallow water equations) resulting from the complete Navier-Stokes three-dimensional equations. This gives a system consisting of one equation for mass continuity and two force-motion equations. The equations are as follows (Rates et al., 1999):

$$\frac{\partial \mathrm{h}}{\partial \mathrm{t}} + u.grad\left(h\right) + hdiv\left(u\right) = 0 \tag{1}$$

$$\frac{\partial \mathrm{h}}{\partial \mathrm{t}} + u.grad\left(h\right) + g\frac{\partial \mathrm{h}}{\partial \mathrm{t}} - \frac{1}{\mathrm{h}} iv\left(vh\,gard\left(u\right)\right) = S_x - g\frac{\partial Z_f}{\partial \mathrm{x}} \tag{2}$$

$$\frac{\partial \mathrm{v}}{\partial \mathrm{t}} + u.grad\left(v\right) + g\frac{\partial \mathrm{h}}{\partial \mathrm{t}} - \frac{1}{\mathrm{h}} dv\left(vh\,gard\left(v\right)\right) = S_y - g\frac{\partial Z_f}{\partial \mathrm{y}} \tag{3}$$

In the above equations, u and v are the velocity components in the Cartesian x and y directions (m/s), h is the depth of flow (m), Z_f stands for bed height (m). S_x and S_y are source terms, g is the gravitational acceleration, and t is time. This model uses a constant eddy viscosity, length mixing, or K-ε turbulence scheme.

2.1.1. Navier-Stokes and Reynolds equations

The Navier-Stokes equations represent mass conservation or continuity equation, which are expressed as follows (Vreugdenhil, 1994).

$$\frac{\sigma}{\sigma t}(\rho u)+\frac{\sigma}{\sigma x}\left(\rho u^2\right)+\frac{\sigma}{\sigma y}(\rho uv)+\frac{\sigma}{\sigma z}(\rho uw)-\rho\int v+\frac{\sigma p}{\sigma x}-\frac{\sigma \tau_{xx}}{\sigma x}-\frac{\sigma \tau_{xy}}{\sigma y}-\frac{\sigma \tau_{xz}}{\sigma z}=0 \quad (4)$$

$$\frac{\sigma}{\sigma t}(\rho v)+\frac{\sigma}{\sigma x}(\rho uv)+\frac{\sigma}{\sigma y}\left(\rho v^2\right)+\frac{\sigma}{\sigma z}(\rho vw)-\rho\int u+\frac{\sigma p}{\sigma y}-\frac{\sigma \tau_{xv}}{\sigma x}-\frac{\sigma \tau_{vv}}{\sigma y}-\frac{\sigma \tau_{vz}}{\sigma z}=0 \quad (5)$$

$$\frac{\sigma}{\sigma t}(\rho w)+\frac{\sigma}{\sigma x}(\rho uw)+\frac{\sigma}{\sigma y}(\rho vw)+\frac{\sigma}{\sigma z}\left(\rho w^2\right)+\frac{\sigma p}{\sigma z}-\rho g-\frac{\sigma \tau_{xz}}{\sigma x}+\frac{\sigma \tau_{vz}}{\sigma y}+\frac{\sigma \tau_{zz}}{\sigma z}=0 \quad (6)$$

where, f is the Coriolis acceleration parameter and obtained from the following equation:

$$f = 2\Omega \sin \Phi \quad (7)$$

Also τ_{ij} is viscosity stress which is defined in terms of fluid deformation rate as follows:

$$\frac{\tau_{ij}}{\rho} = \nu\left(\frac{\sigma u_i}{\sigma x_i}+\frac{\sigma u_j}{\sigma x_i}\right) \quad (8)$$

where ν is a kinematic viscosity.

The general form of the equation is obtained by applying the principle of mass conservation to the volumetric element of the fluid as follows (Berger and Stockstill, 1995).

$$\frac{\sigma p}{\sigma t}+\frac{\sigma}{\sigma}(\rho u)+\frac{\sigma}{\sigma}(\rho v)+\frac{\sigma}{\sigma z}(\rho w)=0 \quad (9)$$

Density of water (ρ) depends on pressure, temperature and salinity. In this condition, considering that the fluid is incompressible and regardless of temperature and salinity changes, a constant density value is assumed:

$$\frac{\sigma \rho}{(t.x.y.z)}=0 \quad (10)$$

Thus, the mass equation becomes simpler:

$$\frac{\sigma u}{\sigma x}+\frac{\sigma v}{\sigma y}+\frac{\sigma w}{\sigma z}=0 \quad (11)$$

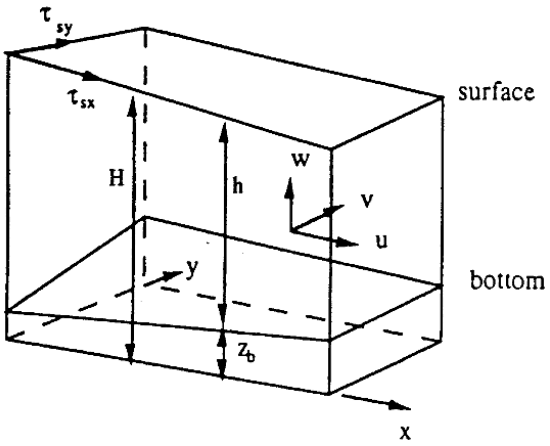

Fig. 1. Definition of coordinate system and boundaries (Berger and Stockstill, 1995)

2.2.Numerical Formulation

2.2.1. The Residual Weighted

The weighted residuals method is one of the most common direct methods of calculating unknown filed variable with solving partial differential equations. In this method, the partial differential equations are estimated by the approximation function $u\hat{}$ as follows:

$$L(u) = f \quad (12)$$

$$\hat{u} = \phi_0 + \sum_{i=1}^{n} c_i \phi_i \quad (13)$$

Where ϕ_i and ϕ_0 are approximation functions. The approximation error is expressed by the following formula:

$$E = L(u) - f \quad (14)$$

The main idea in using the weighted residual method is to minimize this error as much as possible. It should be noted that the value of approximate field nodes in computing of the residual Error (E) is not the same as each other. Therefore, the unknown coefficients

C_i are determined by considering the following integrals equal to zero*:*

$$\int_{\Omega} W_i E \, d\Omega = 0 \quad (i = 1.\cdots.n) \tag{15}$$

where Ω is the domain and W_i is the weight functions*.* In Galerkin method, which is one of the common weighted methods, weight values are taken equal to approximation functions, i.e*:*

$$W_i = \phi_i \tag{16}$$

In the following section, the weighted residual form the governing equations will be determined.

2.2.2. The Residual Weighted Form of the Continuity Equation

The continuity equation in its weighted residual form is as the follows:

$$f_c = \int W_i \left(\frac{\sigma h}{\sigma t} + h\frac{\sigma u}{\sigma x} + h\frac{\sigma v}{\sigma y} + u\frac{\sigma h}{\sigma x} + v\frac{\sigma h}{\sigma y} - I\right) d = 0 \tag{17}$$

In this equation h, u, and v are the approximate values of $\hat{h}$, $\hat{u}$ and $\hat{v}$ respectively.

Equation (17) can be written as follows

$$f_c = \int W_i \frac{\sigma h}{\sigma t} d + \int W_i h \frac{\sigma u}{\sigma x} d + \int W_i h \frac{\sigma v}{\sigma y} d + \int W_i u \frac{\sigma h}{\sigma x} d + \int W_i v \frac{\sigma h}{\sigma y} d - \int W_i I d = 0 \tag{18}$$

2.2.3. Discretization of Equations by FEM

In order to spatially discrete the equations, the domain is divided into triangular elements with three nodes. The unknown variables h, u and v are approximated by the linear shape functions in each element based on the values of the unknowns in the nodes. As it mentioned before, due to the usage of Galerkin method, weight functions (W_i) are equal to shape functions (N_i), and thus the following equations are obtained:

$$h = \sum_{i=1}^{NN} N_i(x,y).h_i(t) \tag{19}$$

$$u = \sum_{i=1}^{NN} N_i(x,y).u_i(t) \tag{20}$$

$$v = \sum_{i=1}^{NN} N_i(x,y).v_i(t) \tag{21}$$

where NN is the total number of nodes, h_i, u_i and v_i are the values of the dependent variables in each node. The form functions N_i are defined in the range Ω corresponding to the form functions $N_i^{(e)}$ in the range of elements, so that the definition of the function in the domain of each element adjacent to node i corresponds to the definition of the function as the form function of node i of that element. In addition, the value of the function in the range of non-adjacent elements of node i is equal to zero and node i is equal to one.

2.2.4. Galerkin Form of the Continuity Equation

The Galerkin form of the continuity equation for node i, is explained as follows:

$$(f_c)_i = (A_1)_i + (A_2)_i + (A_3)_i + (A_4)_i + (A_5)_i + (A_6)_i = 0 \tag{22}$$

$$(A_1)_i = \sum_e \sum_{i=1}^{3} \frac{\sigma h_i}{\sigma t}_i (P_1)_{i,j} \tag{23}$$

$$(A_2)_i = \sum_e \sum_{j=1}^{3} \sum_{k=1}^{3} h_j u_k (P_2)_{i,j,k} \tag{24}$$

$$(A_3)_i = \sum_e \sum_{j=1}^{3} \sum_{k=1}^{3} h_j v_k (P_3)_{i,j,k} \tag{25}$$

$$(A_4)_i = \sum_e \sum_{j=1}^{3} \sum_{k=1}^{3} u_j h_k (P_2)_{i,j,k} \tag{26}$$

$$(A_5)_i = \sum_e \sum_{j=1}^{3} \sum_{k=1}^{3} v_j h_k (P_3)_{i,j,k} \tag{27}$$

$$(A_6)_i = \sum_e I (P_6)_i \tag{28}$$

It should be noted that a set of equations will be appeared which is solved by removing Gauss method.

2.3.Conceptual Model

2.3.1. Boundary conditions

A dynamic flood event that occurred on January 8, 1996 is considered for simulation. Boundary conditions include upstream and downstream are considered as flow rate and water level elevation, respectively. This boundary condition creates the problem of no circulation in the downstream. In order to keep the solution of differential equations constant, there is a need for boundary conditions.

In order to solve shallow water equations, boundary conditions in the bed floor are required first. Boundary conditions at the surface and bed floor are divided into two categories: cinematic conditions and dynamic conditions, each of which are as follows (Abril, 2002; Gee et al., 1990)

2.3.2. Kinematic boundary conditions

These conditions indicate the fact that water particles are not able to move and they are fixed. For a fixed boundary, this means that the vertical component of velocity must be zero (Abril, 2002).

$$u\frac{\sigma z_b}{\sigma x}+v\frac{\sigma z_b}{\sigma y}-w=0 \qquad (29)$$

$$at \quad z=z_b$$

On the free surface this issue is a bit more complicated because the free surface is changing and moving. Therefore, the relative velocity perpendicular to the surface must be zero, i.e:

$$\frac{\sigma H}{\sigma t}+u\frac{\sigma H}{\sigma x}+v\frac{\sigma H}{\sigma y}-w=0 \qquad (30)$$

$$at \quad z=H$$

2.3.3. Dynamic boundary conditions

These conditions are about the forces enforced by the edges on the fluid. In the floor, it can be assumed that the viscous fluid adheres to the floor, i.e: (Abril, 2002):

$$u=v=0 \qquad (31)$$

which is known as dynamic conditions. At the free surface, the continuity of the stresses is taken into account, in other words the stresses below of free surface is equal to the air stresses above it. In fact, surface tension is no longer exist, therefore:

$$p=p_a \qquad (32)$$

where p_a is the atmospheric pressure.

Shear stresses may be applied by the wind. The amount of these shear stresses $(\tau_{sx}.\tau_{sy})$ depends to the surface water and it is obtained from the following equation:

$$\tau_{sx}=-\tau_{xx}\frac{\sigma H}{\sigma x}-\tau_{xy}\frac{\sigma H}{\sigma y}+\tau_{xz} \qquad (33)$$

$$at \quad z=H$$

A similar relation can be obtained for the y direction (Anderson et al., 2015)

2.4.Model Setup

2.4.1. Case Study

A wide river with dimension of 50 m*10 m and a maximum flow rate of 1 m^3 is considered. Generated meshes for this river are shown in Figure 2. Three direct stations (A1 series), 60 degrees (B21 series) and 110 degrees (B39 series) presented in Table 1, have been selected for investigation as samples (Gee et al., 1990).

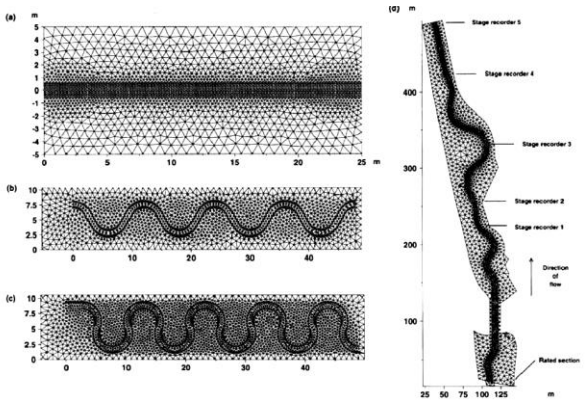

Fig. 2. Study area (Gee et al., 1990)

Table 1- Specifications of the study area (Gee et al., 1990)

Criteria	A1	B21	B39
Total width (meters)	10	10	10
Channel base width (meters)	1.5	0.9	0.9
Channel depth	0.15	0.15	0.15
Channel slope	1:1	1:1	1:1
Channel top width (meters)	1.8	1.2	1.2
Width (meters)	¼	Variable	Variable
Input conditions	Discharge	Discharge	Discharge
Output conditions	Fixed stage	Fixed stage	Fixed stage
Manning coefficient	0.01	0.01	0.01

3. Results and Discussion

Results presented that the two-dimensional finite element model with simple turbulence is able to predict hydraulic parameters such as flow rate and height accurately in cross sections. This means that even in a three-dimensional condition with lateral velocity near the canal, the model is able to show the

momentum transfer between the main canal and the floodplain sufficiently. Comparison between FEM results and observation data (field data) indicates the accuracy and strength of FEM in simulation procedure. Figure 3-5 shows this comparison.

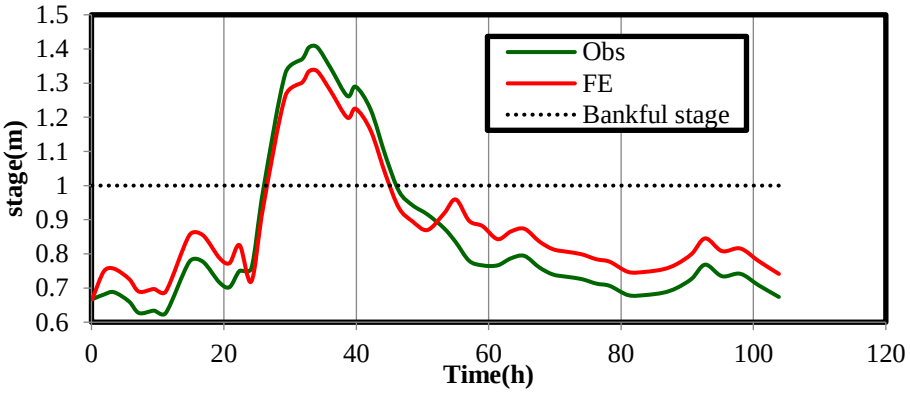

Fig. 3. Comparison of the FEM hydrograph and the observational data at the station 1

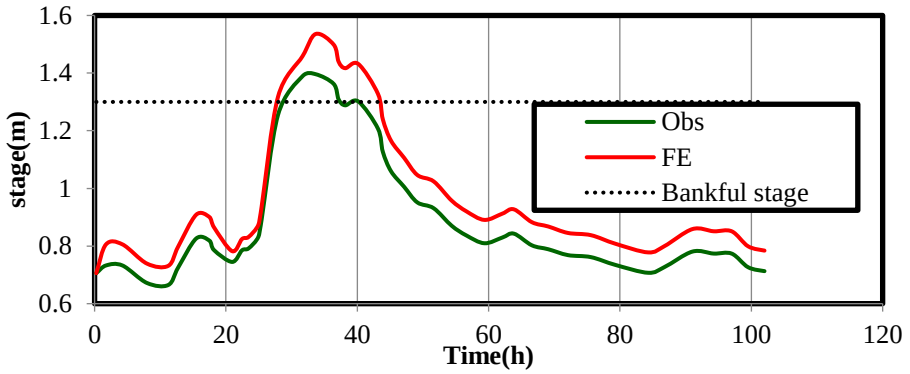

Fig. 4. Comparison of the FEM hydrograph and the observational data at the station 2

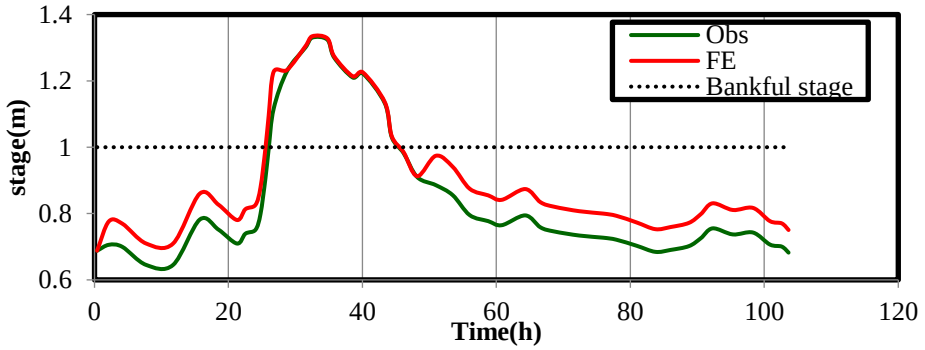

Fig. 5. Comparison of the FEM hydrograph and the observational data at the station 3

Simulation was performed to determine the river hydrograph in three locations. A1, B21 and B39 are three locations. Figure 3 is depicted for A1, Figure 4 and figure 5 are for B29 and B31 locations, respectively.

In A1 section, the difference between observation and finite element method results are quite obvious, this difference exists in the whole hydrograph even in the peak of the flow. These two graphs are corresponded to each other between 40 and 55 hrs. In B21 section, (figure 4), the closeness of two graphs is happened between 20 and 30 hr, however in the rest of times, the difference exists. It should be noticed that the difference between two graphs in figure 4 is lower than figure 3 and finite element is more accurate in this location.

In B39 location, (figure 5), FEM and observation data have a complete correspondence to each other between 20 and 40 hr. This period of time is near to peak of flow. Totally, as it can be seen, the correspondence of the finite element result and observation data are obvious. In the outlet

location, there were three calibration datasets which each of them has the data of water level, flow rate, and peak flow. As a result, only the peak point time is going to accurately predicted.

The water level is achieved for three different locations. This parameter is achieved with two different methods, Manning and FEM. Figure 6, 7, and 8 are depicted the results of these two methods.

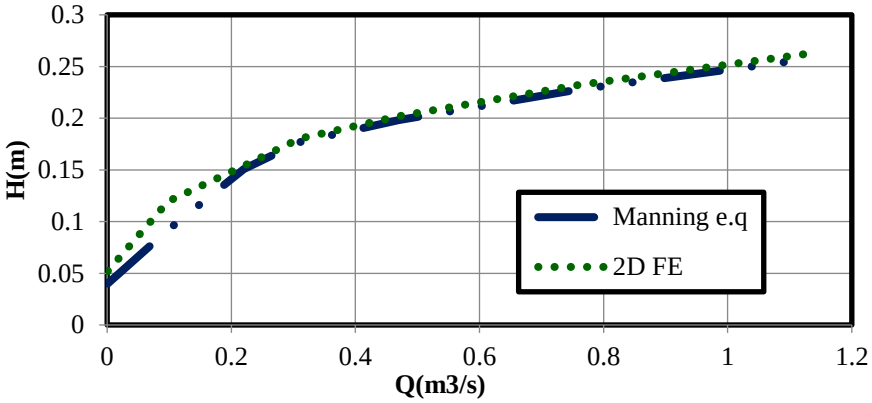

Fig. 6. Comparison of observational flow curves with FEM predictions and Manning equation at the Station No. 1

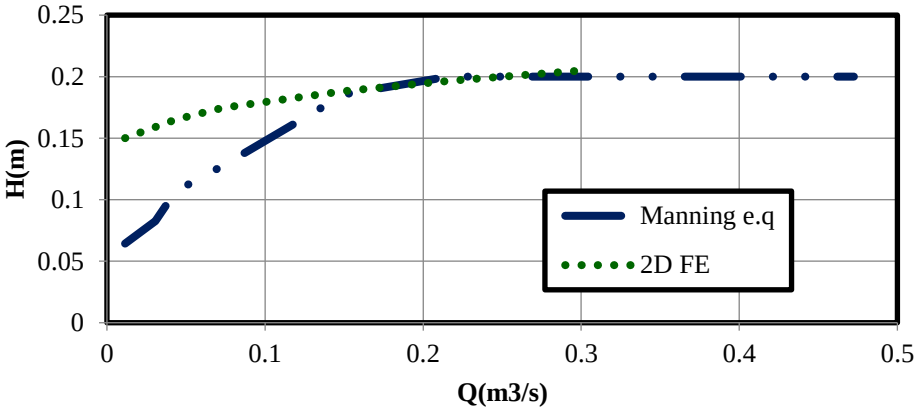

Fig. 7. Comparison of observation flow curves with FEM predictions and Manning equation at the station No. 2

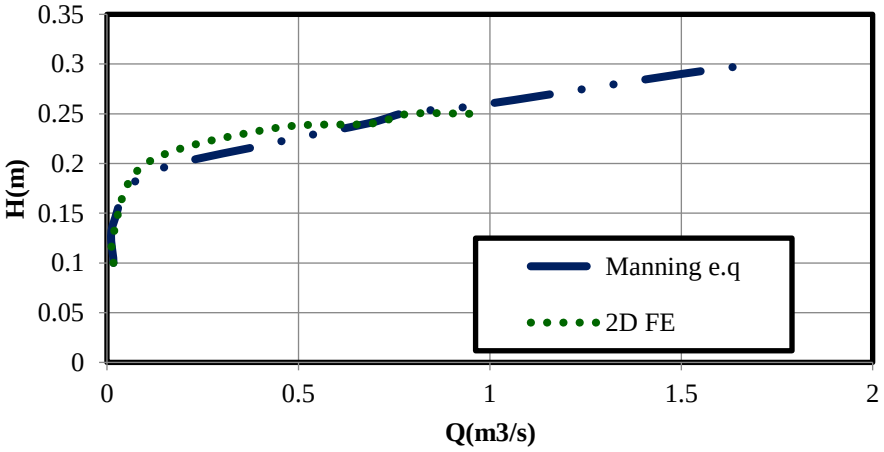

Fig. 8. Comparison of observational flow curves with FEM predictions and Manning equation at the station No. 3

As it clear, the correspondence of FE water level is really high to the Manning water level, and this fact shows the performance of FEM in order to simulation of water level. However, in figure 7 which stands for B21 location, the difference of water level in the first values of

flow rate is quite high, but this difference is decreasing gradually with moving to high flow rates.

3.1.Evaluation of the performance of FEM

Mean Error (ME), Mean Absolute Error (MAE) and Root Mean Square Error (RMSE) were used as criteria for determining the performance of the model. Results are illustrated in Table 2.

Table 2- Calculation of Mean Error, Mean Absolute Error and Root Mean Square Error (m)

Error criteria	Station 3	Station 2	Station 1
ME	0.125	0.110	0.195
MAE	0.198	0.211	0.175
RMSE	0.211	0.253	0.224

According to the Table (2), the value of the root mean square error is in the acceptable range, so the method used for simulation is efficient and accurate. It should be noted that the proposed model in addition to its advantageous including, high accuracy and low computational cost, it has some limitation in domains with irregular geometry. This model in the irregular boundaries show some drawbacks that may lead to errors.

4. Conclusion

Using the principle of mass conservation and its application to volumetric elements, the continuity equation for compressible fluid is obtained, which, assuming the volume mass constant (ρ = constant), becomes a simple and well-known continuity equation. Applying the principle of motion size survival to the volumetric element also gives the motion size equations or Navier-Stokes in three directions. Using the principle of energy conservation in a simplified case, we arrive at the Bernoulli relation. The Bernoulli equation or integration of motion size equations in frictionless flow (Euler equation) is also achievable, so finding all unknowns does not require all three of the above equations, and in practice the continuity and motion equations (Navier-Stokes equations) are usually used. For this purpose, the governing equations of shallow water flow are first extracted from the basic hydrodynamic equations (continuity and Navier-Stokes) and the governing assumptions and types of boundary conditions are described. In the next step, the spatial separation of the equations is done by the finite element method and based on the Galerkin method (one of the weighted residual methods), for which the linear and triangular isometric parametric elements are used. Results showed that the proposed model is able to predict accurately the hydraulic parameters such as height and flow rate. This is due to the closeness of observation data and FDM results.

5. Disclosure statement

No potential conflict of interest was reported by the authors

6. References

Abril, J. B. (2002). Overbank flood routing analysis applying jointly variable parameter diffusion and depth-averaged flow finite element models. *Proceedings of the International Conference on Fluvial Hydraulics*. Belgium. 161-167.

Anderson, M., Woessner, W., & Hunt, R. (2015), Applied Groundwater Modeling Second Edition: *Simulation of Flow and advective Transport in 2nd*. Academic Press, 133-135.

Ayoubzadeh, S. A., & Zahiri, A. (2003). New method of envelope sections in studying of flow hydraulics of river compound channels using 2-D model. *International Journal of Engineering Science*. 14(2), 103-116. (In Persian)

Barzegaran, M., Mehdizadeh, H., & Pour Esmail, S. (2017). Numerical analysis of bed sediment with shallow water equations using reinforced Riemann method, *2nd International Conference on Civil Engineering, Architecture and Crisis Management*, Tehran.

Bates, P. O., Hervouet, J. M., & Anderson, M. G., (1994). Computation of a flood event using a two dimensional finite element model and its comparison to field data. *American Society of Civil Engineers*, New York, 243-256.

Behzadi, F., & Newman III, J. C. (2020). An exact source-term balancing scheme on the finite element solution of shallow water equations. *Computer Methods in Applied Mechanics and Engineering*, 359, 112662.

Berger R. C. & Stockstill R. L. (1995). Finite-Element Model for High-Velocity Channel. *Journal of Hydraulic Engineering*, 121(10), 710-716.

Deymevar, S and Akbarpour, A. (2017). *Modeling Dam Failure Using Petrov-Galerkin*

meshless Method and Shallow Water Equations, Master Thesis, University of Birjand, Birjand, Iran.

Fread, D. L. (1985). Channel routing. *Hydrological forecasting/edited by MG Anderson and TP Burt.*

Gee, D.M., Anderson, M.G., & Baird, L. (1990). Large scale floodplain modelling Earth Surface, *Processes and Landforms*, 15,512-523

Ghobadian, R., & Mehrmousavi, Z. (2019). Numerical Simulation of Strip Irrigation Using Solving Shallow Water Equations in Two-Dimensional Line Curve Coordinates, *First International Congress and Fourth National Iranian Irrigation and Drainage Congress, Urmia*.

Izem, N., & Seaid, M. (2021). A well-balanced Runge-Kutta discontinuous Galerkin method for multilayer shallow water equations with non-flat bottom topography. *Advances in Applied Mathematics and Mechanics*. 14(3): 725-758.

Khorashadizadeh, M., Azizyan, G., Hashemimanfared, S. A., & Akbarpour, A. (2018). Sensitivity analysis of two-dimensional pollution transport model parameters in shallow water using RSA method. *Iranian Journal Soil Water Research*, 49(5), 1119-1129.

Rates, P.D., & Wilson, C.A.M.E., Hervouet, J. M., & Stewart, M. D. (1999). Two dimensional finite element modelling of floodplain flow, *Environment*, 85(3-4), 82-88.

Shiono, K., & Knight, D.W. (1991). Turbulent open-channel flows with variable depth across the channel. *Journal of Fluid Mechanic*. 222, 617-646.

Vreugdenhil, C. B. (1994). Numerical Methods for Shallow-Water Flow (Vol. 13). Springer Science & Business Media.